ACS OMEGA

http://pubs.acs.org/journal/acsodf

Article

Thermal Characteristics of Ash from Bamboo and Masson Pine Blends: Influence of Mixing Ratio and Heating Rate

Jianfei Yang, Zixing Feng, Liangmeng Ni, Qi Gao, Yuyu He, Yanmei Hou, and Zhijia Liu*

Cite This: *ACS Omega* 2021, 6, 7008−7014

Read Online

ACCESS | Metrics & More | Article Recommendations

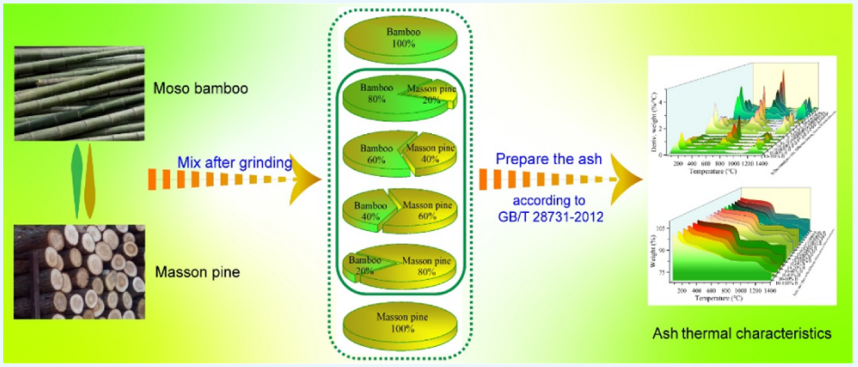

ABSTRACT: Thermal characteristics and kinetic parameters of ash from bamboo and masson pine blends with different mixing ratios were investigated using a thermogravimetric analyzer at different heating rates. The results showed that bamboo ash had lower fusion temperatures than the ash of masson pine. Mixing ratios and heating rates had a significant impact on the thermal characteristics and activation energy of ash samples. There was a synergistic interaction of chemical compositions in the bamboo and masson pine ashes. The mass loss of ash samples increased with the increase in the bamboo content of the blends. All ash samples had the maximum activation energy at the heating rate of 20 °C/min. The activation energy had a good linear correlation with mixing ratios at high conversion and heating rates. The optimum blend was suggested as 20% bamboo/80% masson pine due to its high activation energy. The results of this study are helpful to design a combustion system of bamboo and masson pine blends.

1. INTRODUCTION

Bamboo and masson pine are two main types of biomass sources, which have a great potential for developing biomass energy in China. Especially for bamboo materials, there are about 50−70% of process wastes due to the unique structure of its hollow.[1] Based on previous research results of our group, bamboo and masson pine had a stable co-firing process and there were no synergistic interactions because of their similar physical and chemical properties.[2,3] However, fuel ash, a by-product in the combustion process, has an important impact on the industrial utilization for energy products. The chemical compositions of ash occur to fusion when the combustion temperatures are higher than the melting temperatures, resulting in slagging, agglomeration, or corrosion of ash. This will bring serious technical safety problems during the combustion process of fuels.[4,5] Compared with coal ash, biomass ash is easier to be released, condensed, adsorbed, and deposited on the heated surface of a boiler furnace due to high content of inorganic salts of alkali metals such as KCl and NaCl. The high contents of K_2O in biomass result in the low ash fusion temperature.[6] Some potassium- and calcium-containing compounds also can react with aluminosilicates in anthracite to produce low-temperature eutectic, thereby reducing the melting temperatures of biomass blends and anthracite.[7] The chemical compositions have a significant influence on the changes of the crystalline phase, formation mechanism, and fusion behavior of ash.[8] The main chemical compositions of bamboo and masson pine ash are significantly different. The major chemical compositions of bamboo ash are K_2O (34.23%), SiO_2 (24.32%), SO_3 (14.05%), MgO (6.69%). However, masson pine ash mainly includes Fe_2O_3 (33.60%), CaO (21.70%), K_2O (7.55%), SO_3 (4.84%), and SiO_2 (4.34%).[9] This results in that bamboo and masson pine ashes have different melting temperatures. The fluid temperature, hemispheric temperature, softening temperature, and deformation temperature (DT) of bamboo ash are 1181.00,

Received: December 28, 2020
Accepted: February 17, 2021
Published: March 3, 2021

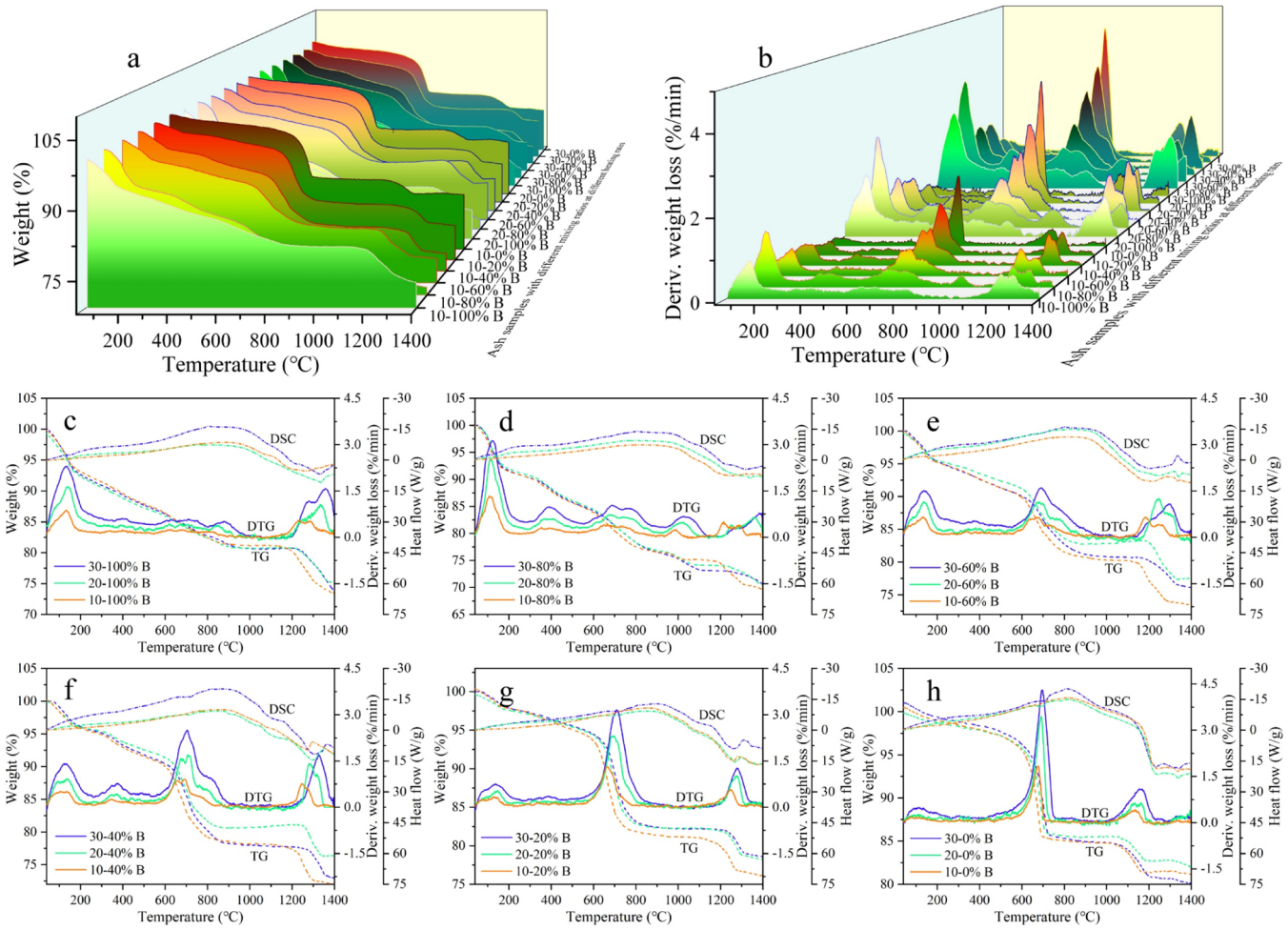

Figure 1. TG−DTG curves of ash samples (a) TG curves; (b) DTG curves; (c) TG−DTG curves of 100% B; (d) TG−DTG curves of 80% B; (e) TG−DTG curves of 60% B; (f) TG−DTG curves of 40% B; (g) TG−DTG curves of 20% B; (h) TG−DTG curves of 0% B.

1136.20, 1038.40, and 949.60 °C, whereas those of masson pine ash are 1230.80, 1160.00, 1110.40, and 1048.20 °C.

The mixing ratios of the blends also affect the ash fusion properties due to different chemical compositions of each feedstock. The mixing ratios of eucalyptus bark/lignite should be controlled within 40% to prevent ash sintering even though there is no linear relationship between ash fusion characteristics of the blends and the mixing ratio.[10] Furthermore, the extracts and volatiles in the ash of biomass and minerals decrease the activation energy and increase the thermal decomposition strength.[11] The activation energy of coal ash is decreased during co-firing of coal and rice straw or cotton stalk.[12] Therefore, the application of biomass leachate can regulate the fusibility of coal ash.[13] The melting point of silicate increases and the slag content decreases when kaolin and calcite are added to corn straw.[14] It is also confirmed that there is a synergistic interaction between different fuel resources. Therefore, the melting characteristics of the ash produced by the mixed fuel depend on the fuel type and mixing ratio during the co-firing process.[15] This made it more difficult to accurately analyze the ash fusion characteristics and mechanism because of the difference of each feedstock.

The preparing temperatures of ash have a significant impact on the content and thermal properties, which is also attributed to the chemical diversity of minerals contained in the biomass.[16] Therefore, the selection of the suitable temperature is very important during the preparation process of biomass ash. Based on the standard method of ash preparation, the temperature selected in the determination of fossil fuel ash is higher than that of biomass ash. For example, the preparing temperature is 815 ± 10 °C according to the standard of solid mineral fuel-determination of ash (ISO 1171:2010). However, the preparing temperature of the standard test method for ash in biomass (E1755-01:2015) is 575 ± 25 °C. The biomass ash should be prepared at the temperature of 550 ± 10 °C according to the standard of proximate analysis of solid biofuels (GB/T 28731-2012). The different temperatures change the chemical composition of biomass ash, which further influences the fusion characteristics. It is a fact that the fusion properties of bamboo or masson pine ash have been reported.[9,17] However, the object of this research is to investigate the thermal characteristics of ash during the co-firing process of bamboo and masson pine and further analyze the influence of the mixing ratio on ash properties. It is very helpful to operate the co-firing system of bamboo and masson pine and develop them for energy products. Based on this motivation, the ash of bamboo and masson pine blends with different mixing ratios was prepared using a digitally controlled GSL 1600X tube furnace with 550 ± 10 °C according to the standard method (GB/T 28731-2012). The synchronous thermal analysis (TG−DSC) was used to determine the thermal behavior of ash. In addition, the non-isothermal model

https://dx.doi.org/10.1021/acsomega.0c06300
ACS Omega 2021, 6, 7008−7014

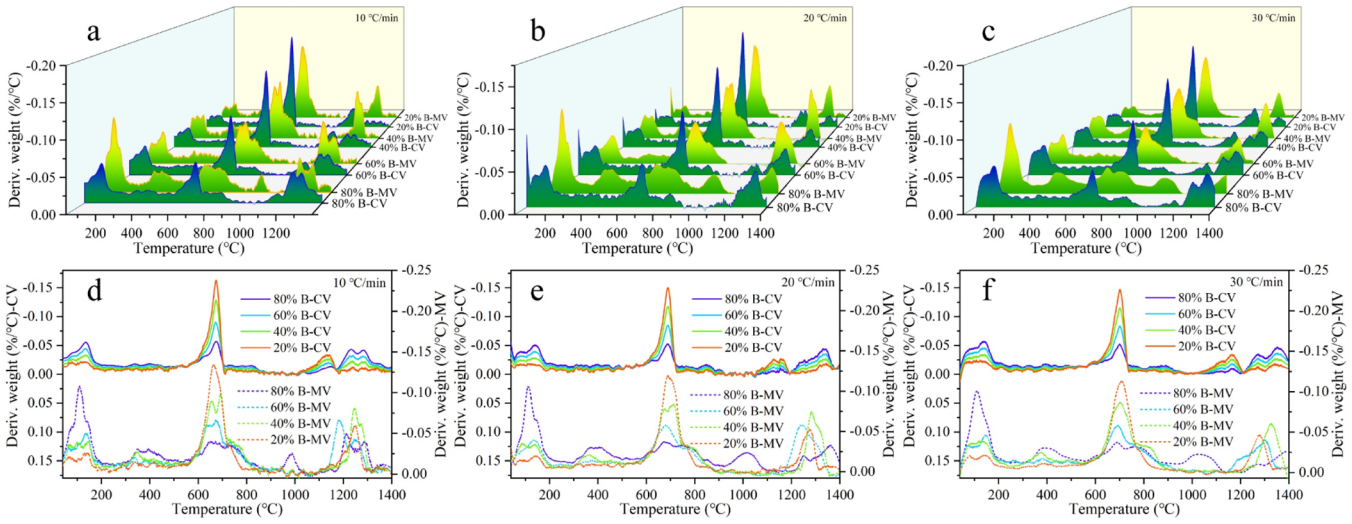

Figure 2. Synergistic interaction of bamboo and masson pine ash (a,d) 10; (b,e) 20; (c,f) 30 °C/min (CV is the calculated value, MV is the measured value).

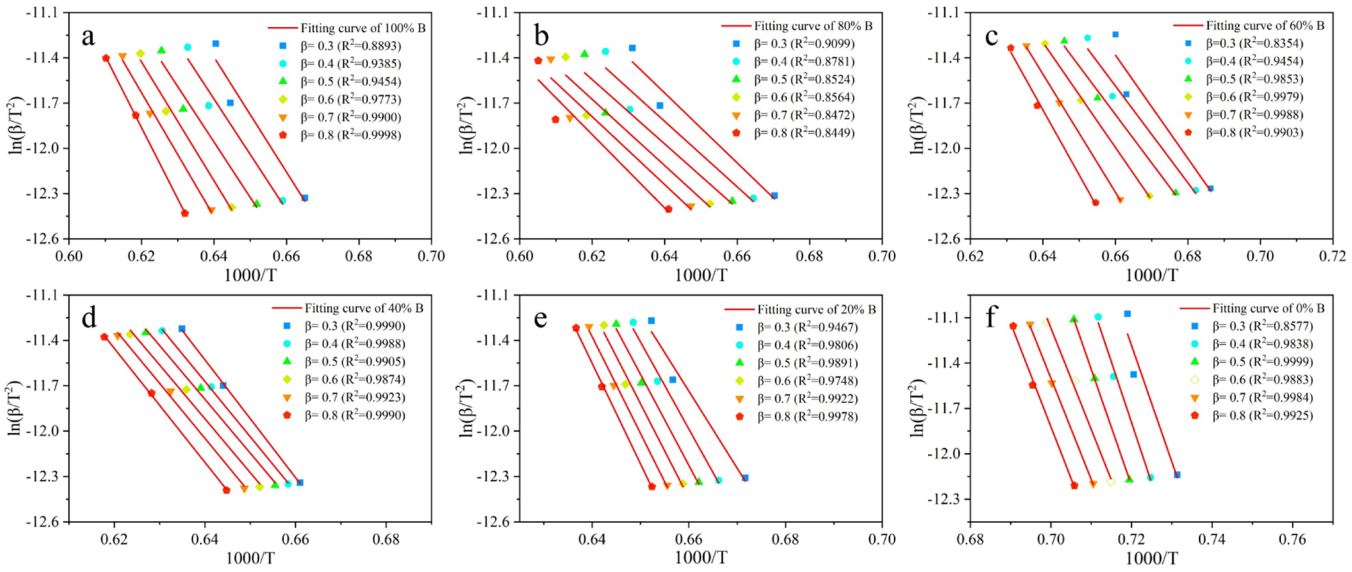

Figure 3. Fitting curve between $\ln(\beta/T^2)$ and $1000/T$ of the KAS model (a) 100% B; (b) 80% B; (c) 60% B; (d) 40% B; (e) 20% B; (f) 0% B.

of the Kissinger−Akahira−Sunose equation (KAS model) and the isothermal model of the Coats−Redfern formula (C−R model) were used to calculate the activation energy of ash fusion.

2. RESULTS AND DISCUSSION

2.1. Thermal Characteristics. The TG−derivative TG (DTG) curves of ash samples of blends with heating rates of 10, 20, and 30 °C/min are showed in Figure 1A,B. The mass loss curve of bamboo ash is nearly coincident at different heating rates during the total thermochemical reaction (Figure 1C). The final mass loss of bamboo ash was about 25.0%. The DTG curve of bamboo ash showed that there were two distinct peaks located at lower and higher temperatures. The first characteristic peak was due to evaporation of water. It is a fact that ash can absorb moisture from the environment because of its pore structure, which leads to a weak mass loss in the DTG curve. The second distinct peak with a temperature of 1250 °C was mainly due to the breakdown and release of complex high-temperature mineral and inorganic species, such as K_2O, SiO_2, Fe_2O_3, and CaO.[18] There were significant differences of TG−DTG curves between masson pine ash and bamboo ash (Figure 1H). In the TG curves of masson pine ash with different heating rates, the mass loss of ash was relatively stable at the low temperature range and then dropped sharply, which was significantly different from that of bamboo ash, showed in Figure 1C. Compared with bamboo ash, masson pine ash was not easier to absorb moisture. As the heating rate increased, the mass loss of masson pine ash slightly increased. The mass loss of ash samples increased with the increase in bamboo content of blends at the same heating rate (Figure 1A). The characteristic peaks of the thermochemical reaction were almost the same for all ash samples, except for 80% B, showed in Figure 1B. The 80% B sample had a mass loss peak at about 1000 °C. This may be due to the formation of new compounds when the ash samples were prepared at 550 °C, which catalyzed the thermochemical reaction of the ash sample. There were three main characteristic peaks in the DTG curve of blend ashes (Figure 1C−G). The first peak located at a

https://dx.doi.org/10.1021/acsomega.0c06300
ACS Omega 2021, 6, 7008−7014

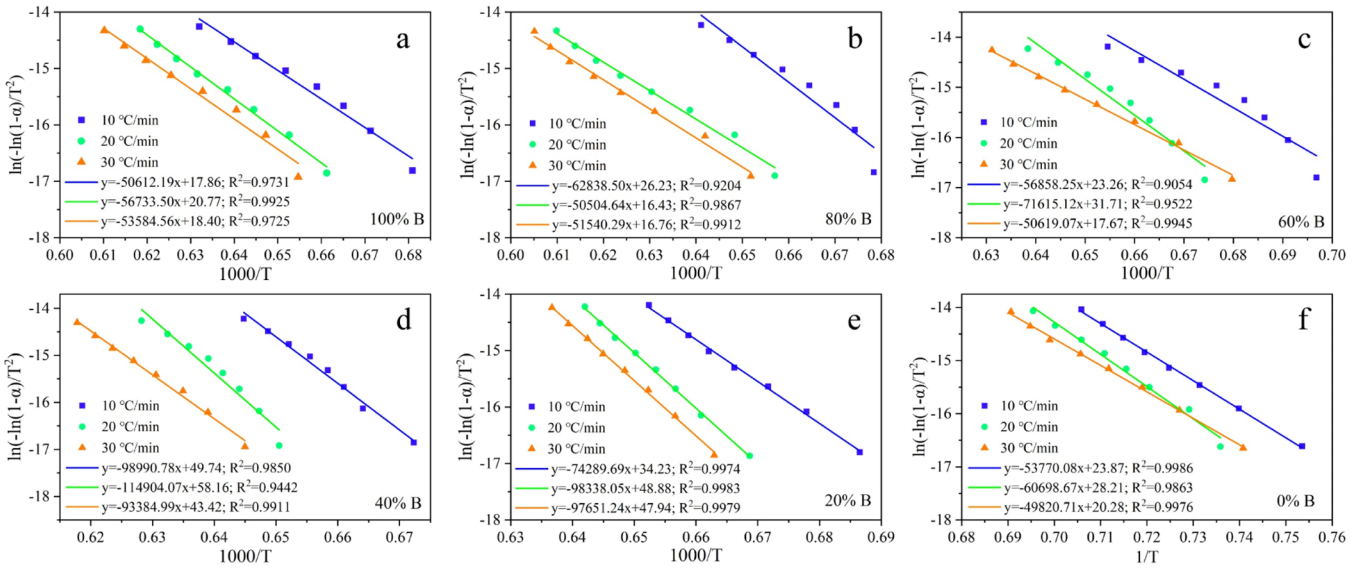

Figure 4. Fitting curve between $\ln[-\ln(1-\alpha)/T^2]$ and $1000/T$ of the C−R model (a) 100% B; (b) 80% B; (c) 60% B; (d) 40% B; (e) 20% B; (f) 0% B.

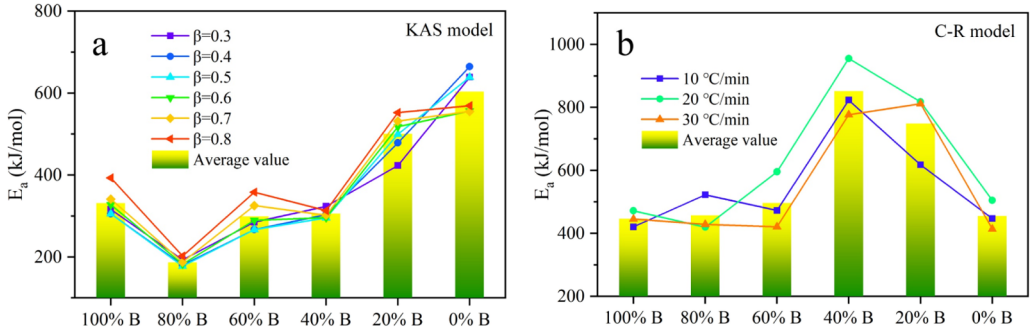

Figure 5. Correlation of activation energy and mixing ratios using (a) C−R and (b) KAS models.

temperature of 50−200 °C was corresponding to evaporation of water from bamboo ash. Furthermore, the maximum of peak gradually decreased when the bamboo content decreased in the blends. Similarly, the second peak located at temperature of 600−800 °C was corresponding to that in the weightlessness peak of masson pine ash. Its maximum of peak gradually decreased with increase in bamboo content of blends. The third peak, located at a temperature of 1200−1400 °C was due to the vaporization of ash after melting. In the previous research,[9] bamboo ash had a low fusion temperature range of 949−1181 °C, corresponding to the initial DT and flow temperature. Masson pine ash had a high fusion temperature range of 1048−1203 °C. This confirmed that the chemical compositions of ash during the co-firing process of bamboo and coal occurred to reaction when the temperature was higher than DT, resulting in the mass loss of the pyrolysis process.[17]

Compared with bamboo alone or masson pine ash, the TG−DTG curves of blend ashes had more characteristic peaks (Figure 1). Some new characteristic peaks were mainly due to the synergistic interaction of chemical compositions in bamboo and masson pine ash. This further confirmed that the mixing ratio had a significant impact on the ash thermal characteristics. Figure 2 shows the difference between the DTG curve of the calculated value and the measured value of the blend ashes. The DTG curves of calculated and measured mass loss did not overlap, indicating that there was a synergistic interaction of bamboo and masson pine ash. It further confirmed that some components of bamboo ash occurred thermal chemical reaction with that of masson pine ash. For example, a higher content of K_2O and Na_2O in bamboo ash could react with a high content of Fe_2O_3 in masson pine ash to produce low-melting substances.[19]

2.2. Kinetic. The equal conversion method is one of the most widely used methods in thermal analysis kinetics. The results of the KAS model are reliable to calculate the activation energy without knowing the specific form of the mechanism function.[20] The KAS model was used to calculate the kinetic parameters of ash samples in this research. The fitting curve between $\ln(\beta/T^2)$ and $1000/T$ is showed in Figure 3. Figure 5A shows that the KAS model had higher R^2 values, indicating that it was suitable to calculate the kinetic of ash samples. Masson pine ash had an obviously higher activation energy than bamboo ash at each conversion rate. The activation energies of masson pine ash were 638.96, 664.87, 638.62, 556.43, 555.35, and 569.32 kJ/mol, corresponding to 0.3, 0.4, 0.5, 0.6, 0.7, and 0.8 of conversion rates. With different conversion rates, the average activation energy of masson pine ash was 603.93 kJ/mol. Similarly, the activation energies of bamboo ash were respectively 316.39, 305.49, 305.34, 327.58, 341.26, and 393.06 kJ/mol. With different conversion rates, the average activation energy of bamboo ash was 331.52 kJ/mol. The higher average activation energy of masson pine ash

https://dx.doi.org/10.1021/acsomega.0c06300
ACS Omega 2021, 6, 7008−7014

indicated that masson pine ash was more difficult to melt, slag, and scale than bamboo ash. This phenomenon was mainly due to the difference of chemical compositions between masson pine and bamboo ash. Bamboo ash had an obviously higher content of K_2O (34.23%) than masson pine ash (7.55%).[9,21] Mu et al. found that some alkali metal aerosols condensed on the surface of the fly ash, either forming a sticky layer or reacting with SiO_2 and Fe_2O_3 to produce low-melting substances.[22] The activation energy of all ash samples increased with the increase of conversion from 0.3 to 0.8 (Figure 5A). However, the activation energy of ash samples gradually increased with a decrease in bamboo content of blends. When bamboo content of blends was higher than 40%, the activation energy of blend ash was lower than that of bamboo alone or masson pine ash. This might be due to the synergistic effect of the chemical components of bamboo and masson pine during the preparation process of the ash sample, which reduced the activation energy. There were good linear correlations of activation energy and mixing ratios. With different conversion rates, the average activation energy of 80% B, 60% B, 40% B, and 20% B were 187.09, 298.68, 305.61, and 500.57 kJ/mol. Ash samples of 20% B had the maximum activation energy with values of 423.31, 478.50, 499.55, 517.96, 531.64, and 552.43 kJ/mol at conversion rates of 0.3, 0.4, 0.5, 0.6, 0.7, and 0.8. The higher activation energies of ash samples indicate a greater barrier to ash slagging, fouling, corrosion, and agglomeration during the combustion process. Therefore, the optimum blend ratio was suggested to be 20% B in this research.

As a classical isothermal model, the C−R model is normally considered to be in accordance with a single reaction kinetic model and the obtained activation energy is generally considered to be the average value of the pyrolysis process.[23] The fitting curve between $\ln[-\ln(1-\alpha)/T^2]$ and $1000/T$ of the C−R model is showed in Figure 4. The high R^2 value also indicated that the C−R model was suitable to evaluate the ash thermal process.[24] The variation of activation energy of bamboo and masson pine ashes was not obvious at different heating rates, corresponding to the average activation energy of 444.99 and 455.30 kJ/mol. The activation energy first increased and then decreased with the decrease in bamboo content of blends. When the bamboo content in the blend was less than 60%, the activation energy of the ash sample was higher than that of bamboo alone or masson pine ash. This might be due to the synergistic interaction of chemical components in the ash samples, thereby increasing the activation energy. At different heating rates, the average activation energies of 80% B, 60% B, 40% B, and 20% B were 456.95, 496.32, 851.57, and 749.03 kJ/mol. The highest activation energy was found to the 40% B, whose activation energies were 823.01, 955.31, and 776.4 kJ/mol at heating rates of 10, 20, and 30 °C/min. The synergistic interaction of chemical compositions obviously increased the activation energies of 40% B and 20% B. All ash samples had the highest values of activation energy at the heating rate of 20 °C/min, except for 80% B, corresponding to 471.68 kJ/mol of bamboo ash, 817.58 kJ/mol of 20% B, 955.31 kJ/mol of 40% B, 595.41 kJ/mol of 60% B, and 504.65 kJ/mol of masson pine ash when the heating rate was 20 °C/min. This suggested that the combustion rate should be 20 °C/min during the co-firing process of bamboo and masson pine. It was confirmed that the activation energy of all ash samples had a good linear correlation with mixing ratios at high heating rates.

3. CONCLUSIONS

The ash thermal characteristics of bamboo and masson pine were obviously different even though they had two main characteristic peaks. Bamboo ash had two distinct peaks corresponding to temperatures of 150 and 1300 °C. However, the peak temperatures corresponding to maximum mass loss of masson pine ash were 750 and 1150 °C. Mixing ratios and heating rates had a significant effect on fusion characteristics of ash samples. The mass loss of ash samples increased with the increase in the bamboo content of the blends. There was a synergistic interaction of bamboo and masson pine ash. The optimum blend was suggested as 20% B and the combustion rate should be 20 °C/min during the co-firing process of bamboo and masson pine.

4. MATERIAL AND METHODS

4.1. Materials. The 4-year-old moso bamboo (*Phyllostachys heterocycla*) was taken from Zhejiang Province, China. The 20-year-old masson pine (*Pinus massoniana* Lamb.) was taken from Anhui Province, China. After natural drying, the moisture contents of moso bamboo and masson pine were, respectively, 6.45 and 10.08%. They were pulverized into particles with the size of 250−425 μm using a Wiley mill. Then, they were dried in an oven at a temperature of 105 °C for 24 h. The bamboo and masson pine particles were uniformly mixed with mass ratios of 100% bamboo, 80% bamboo, and 20% masson pine, 60% bamboo and 40% masson pine, 40% bamboo and 60% masson pine, 20% bamboo and 80% masson pine, and 100% masson pine. Ash samples of the blends were prepared using a digitally controlled GSL 1600X tube furnace in an air atmosphere at 550 °C according to the standard method of GB/T 28731-2012,[8] labeled as 100% B, 80% B, 60% B, 40% B, 20% B, and 0% B.

4.2. Determination of Ash Thermal Characteristics. TG analysis is widely employed for quickly and reliably evaluating the thermal reaction and kinetics of carbonaceous materials.[25] In this research, the thermal characteristics of ash samples were determined by a synchronous thermal analyzer (SDT-Q600, TA). Ash samples were evenly and loosely distributed in an open pan with an initial mass of about 6−8 mg. The temperature variation was controlled from room temperature (30 ± 5) to 1400 °C with a heating rate of 10, 20, and 30 °C/min, respectively. High-purity nitrogen was used as the balance gas with a flow rate of 50 mL/min. Three replicates of each experiment were performed. The synergistic interaction of bamboo and masson pine ash was calculated by eq 1.

$$M_{\text{calculated}} = M_{\text{bamboo ash}} \times R_{\text{bamboo ash content}} + M_{\text{masson pine ash}} \times R_{\text{masson pine ash content}} \quad (1)$$

where $M_{\text{calculated}}$ is the mass loss of blend ash, $M_{\text{bamboo ash}}$ is the mass loss of bamboo ash, $R_{\text{bamboo ash content}}$ is the bamboo content of the blends, $M_{\text{masson pine ash}}$ is the mass loss of masson pine ash, and $R_{\text{masson pine ash content}}$ is the content of masson pine in the blends.

4.3. Calculating the Kinetic. Kinetic models are usually divided into isothermal models and non-isothermal models. The kinetic of ash was calculated using the non-isothermal model of KAS equation (KAS model).[26] The C−R formula (C−R model) is a isothermal model, which calculates the kinetic based on different heating rates.[27]

https://dx.doi.org/10.1021/acsomega.0c06300
ACS Omega 2021, 6, 7008−7014

The KAS model mainly uses the specific conversion based on the integral reaction model: $g(\alpha) = \alpha/(1-\alpha)$, where $g(\alpha)$ is usually constant only considering the first-order of this study.[2]

$$\ln(\beta/T^2) = \ln\left(\frac{A\cdot E_a}{R\cdot g(\alpha)}\right) - \frac{E_a}{R\cdot T} \quad (2)$$

where β is the heating rate (°C/min), T is the absolute temperature (K), A is the pre-exponential factor (s^{-1}), E_a is the activation energy (J/mol), and R is the universal gas constant (J/(mol·K)). α is the degree of conversion at time t, which can be calculated by the following equation.

$$\alpha = (m_0 - m_t)/(m_0 - m_\infty) \quad (3)$$

where m_t is the mass of the samples at any time, m_0 is the initial mass of the samples, and m_∞ is the mass of the samples at the end of pyrolysis.

By plotting $\ln(\beta/T^2)$ versus $1/T$, the activation energy (E_a) and pre-exponential factor (A) are obtained through regression analysis.[21,28]

The C−R model can calculate the frequency factor and reaction order by using the activation energy.

$$\ln[-\ln(1-\alpha)/T^2] = \ln\left[\frac{A\cdot R}{\beta\cdot E_a}\left(1 - \frac{2R\cdot T}{E_a}\right)\right] - \frac{E_a}{R\cdot T} \quad (n = 1) \quad (4)$$

where β is the heating rate (°C/min), T is the absolute temperature (K), A is the pre-exponential factor (s^{-1}), E_a is the activation energy (J/mol), R is the universal gas constant (J/(mol·K)), and α is the degree of conversion at time t.

By substituting the common solid reaction mechanism functions into eq 3 and plotting $\ln[-\ln(1-\alpha)/T^2]$ versus $1/T$, E_a and A of the samples are obtained.

AUTHOR INFORMATION

Corresponding Author

Zhijia Liu − *International Centre for Bamboo and Rattan, Beijing 100102, China; Key Laboratory of National Forestry and Grassland Administration/Beijing for Bamboo & Rattan Science and Technology, Beijing 100102, China;* orcid.org/0000-0002-3468-9315; Phone: 86-10-84789869; Email: Liuzj@icbr.ac.cn

Authors

Jianfei Yang − *International Centre for Bamboo and Rattan, Beijing 100102, China; Key Laboratory of National Forestry and Grassland Administration/Beijing for Bamboo & Rattan Science and Technology, Beijing 100102, China;* orcid.org/0000-0002-5686-7223

Zixing Feng − *International Centre for Bamboo and Rattan, Beijing 100102, China; Key Laboratory of National Forestry and Grassland Administration/Beijing for Bamboo & Rattan Science and Technology, Beijing 100102, China*

Liangmeng Ni − *International Centre for Bamboo and Rattan, Beijing 100102, China; Key Laboratory of National Forestry and Grassland Administration/Beijing for Bamboo & Rattan Science and Technology, Beijing 100102, China*

Qi Gao − *International Centre for Bamboo and Rattan, Beijing 100102, China; Key Laboratory of National Forestry and Grassland Administration/Beijing for Bamboo & Rattan Science and Technology, Beijing 100102, China*

Yuyu He − *International Centre for Bamboo and Rattan, Beijing 100102, China; Key Laboratory of National Forestry and Grassland Administration/Beijing for Bamboo & Rattan Science and Technology, Beijing 100102, China*

Yanmei Hou − *International Centre for Bamboo and Rattan, Beijing 100102, China; Key Laboratory of National Forestry and Grassland Administration/Beijing for Bamboo & Rattan Science and Technology, Beijing 100102, China*

Complete contact information is available at: https://pubs.acs.org/10.1021/acsomega.0c06300

Notes

The authors declare no competing financial interest.

ACKNOWLEDGMENTS

This research was financially supported by the "National Key R&D Program of China" (2017YFD0600804).

REFERENCES

(1) Yu, D.; Tan, H.; Ruan, Y. A future bamboo-structure residential building prototype in China: Life cycle assessment of energy use and carbon emission. *Energy Build.* **2011**, *43*, 2638−2646.

(2) Liang, F.; Wang, R.; Jiang, C.; Yang, X.; Zhang, T.; Hu, W.; Mi, B.; Liu, Z. Investigating co-combustion characteristics of bamboo and wood. *Bioresour. Technol.* **2017**, *243*, 556−565.

(3) Mi, B.; Liu, Z.; Hu, W.; Wei, P.; Jiang, Z.; Fei, B. Investigating pyrolysis and combustion characteristics of torrefied bamboo, torrefied wood and their blends. *Bioresour. Technol.* **2016**, *209*, 50−55.

(4) Vassilev, S. V.; Baxter, D.; Andersen, L. K.; Vassileva, C. G. An overview of the composition and application of biomass ash. Part 1. Phase−mineral and chemical composition and classification. *Fuel* **2013**, *105*, 40−76.

(5) Niu, Y.; Tan, H.; Hui, S. e. Ash-related issues during biomass combustion: Alkali-induced slagging, silicate melt-induced slagging (ash fusion), agglomeration, corrosion, ash utilization, and related countermeasures. *Prog. Energy Combust. Sci.* **2016**, *52*, 1−61.

(6) Jandačka, J.; Malcho, M.; Ochodek, T.; Koloničný, J.; Holubčík, M. The increase of silver grass ash melting temperature using additives. *Int. J. Renew. Energy Resour.* **2015**, *5*, 258−265.

(7) Lu, G.; Zhang, K.; Cheng, F. The fusion characteristics of ashes from anthracite and biomass blends. *J. Energy Inst.* **2018**, *91*, 797−804.

(8) Niu, Y.; Du, W.; Tan, H.; Xu, W.; Liu, Y.; Xiong, Y.; Hui, S. Further study on biomass ash characteristics at elevated ashing temperatures: The evolution of K, Cl, S and the ash fusion characteristics. *Bioresour. Technol.* **2013**, *129*, 642−645.

(9) Liu, Z.; Zhang, T.; Zhang, J.; Xiang, H.; Yang, X.; Hu, W.; Liang, F.; Mi, B. Ash fusion characteristics of bamboo, wood and coal. *Energy* **2018**, *161*, 517−522.

(10) Chen, M.; Yu, D.; Wei, Y. Evaluation on ash fusion behavior of eucalyptus bark/lignite blends. *Powder Technol.* **2015**, *286*, 39−47.

(11) Mallick, D.; Poddar, M. K.; Mahanta, P.; Moholkar, V. S. Discernment of synergism in pyrolysis of biomass blends using thermogravimetric analysis. *Bioresour. Technol.* **2018**, *261*, 294−305.

(12) Wei, J.; Guo, Q.; Ding, L.; Gong, Y.; Yu, J.; Yu, G. Understanding the effect of different biomass ash additions on pyrolysis product distribution, char physicochemical characteristics, and char gasification reactivity of bituminous coal. *Energy Fuels* **2019**, *33*, 3068−3076.

(13) Wang, J.; Liu, X.; Guo, Q.; Wei, J.; Chen, X.; Yu, G. Application of biomass leachate in regulating the fusibility of coal ash. *Fuel* **2020**, *268*, 117338.

(14) Xiong, S.; Burvall, J.; Örberg, H.; Kalen, G.; Thyrel, M.; Öhman, M.; Boström, D. Slagging characteristics during combustion of corn stovers with and without kaolin and calcite. *Energy Fuels* **2008**, *22*, 3465−3470.

(15) Vassilev, S. V.; Baxter, D.; Vassileva, C. G. An overview of the behaviour of biomass during combustion: Part II. Ash fusion and ash formation mechanisms of biomass types. *Fuel* **2014**, *117*, 152−183.
(16) Dzurenda, L.; Pňakovič, L. Influence of the burning temperature of the non-volatile combustible content of wood and bark of plantation-grown, fast-growing tree species upon ash production, and its properties in terms of fusibility. *BioResources* **2016**, *11*, 6464−6476.
(17) Liu, Z.; Feng, Z.; Xiang, H.; Yang, J.; Zhang, J. The ash fusion characteristics of bamboo and coal co-firing process. *J. Therm. Anal. Calorim.* **2020**, 1−8.
(18) Kim, J.-H.; Kim, G.-B.; Jeon, C.-H. Prediction of correlation between ash fusion temperature of ASTM and Thermo-Mechanical Analysis. *Appl. Therm. Eng.* **2017**, *125*, 1291−1299.
(19) Wang, X.; Liu, Y.; Tan, H.; Ma, L.; Xu, T. Mechanism research on the development of ash deposits on the heating surface of biomass furnaces. *Ind. Eng. Chem. Res.* **2012**, *51*, 12984−12992.
(20) Damartzis, T.; Vamvuka, D.; Sfakiotakis, S.; Zabaniotou, A. Thermal degradation studies and kinetic modeling of cardoon (Cynara cardunculus) pyrolysis using thermogravimetric analysis (TGA). *Bioresour. Technol.* **2011**, *102*, 6230−6238.
(21) Wang, G.; Zhang, J.; Shao, J.; Liu, Z.; Wang, H.; Li, X.; Zhang, P.; Geng, W.; Zhang, G. Experimental and modeling studies on CO2 gasification of biomass chars. *Energy* **2016**, *114*, 143−154.
(22) Mu, L.; Cai, J.; Chen, J.; Ying, P.; Li, A.; Yin, H. Further study on ash deposits in a large-scale wastewater incineration plant: ash fusion characteristics and kinetics. *Energy Fuels* **2015**, *29*, 1812−1822.
(23) Wang, R.; Liang, F.; Jiang, C.; Jiang, Z.; Wang, J.; Fei, B.; Nan, N.; Liu, Z. Pyrolysis kinetics of moso bamboo. *Wood Fiber Sci.* **2018**, *50*, 77−87.
(24) Mishra, R. K.; Sahoo, A.; Mohanty, K. Pyrolysis kinetics and synergistic effect in co-pyrolysis of Samanea saman seeds and polyethylene terephthalate using thermogravimetric analyser. *Bioresour. Technol.* **2019**, *289*, 121608.
(25) Wei, J.; Guo, Q.; Gong, Y.; Ding, L.; Yu, G. Effect of biomass leachates on structure evolution and reactivity characteristic of petroleum coke gasification. *Renewable Energy* **2020**, *155*, 111−120.
(26) Anca-Couce, A.; Berger, A.; Zobel, N. How to determine consistent biomass pyrolysis kinetics in a parallel reaction scheme. *Fuel* **2014**, *123*, 230−240.
(27) Naqvi, S. R.; Tariq, R.; Hameed, Z.; Ali, I.; Naqvi, M.; Chen, W.-H.; Ceylan, S.; Rashid, H.; Ahmad, J.; Taqvi, S. A.; Shahbaz, M. Pyrolysis of high ash sewage sludge: Kinetics and thermodynamic analysis using Coats-Redfern method. *Renewable energy* **2019**, *131*, 854−860.
(28) Tanner, J.; Bhattacharya, S. Kinetics of CO_2 and steam gasification of Victorian brown coal chars. *Chem. Eng. J.* **2016**, *285*, 331−340.

https://dx.doi.org/10.1021/acsomega.0c06300
ACS Omega 2021, 6, 7008−7014